International Journal of Advances in Electrical Engineering

E-ISSN: 2708-4582
P-ISSN: 2708-4574
IJAEE 2024; 5(2): 06-15

www.electricaltechjournal.com
Received: 07-05-2024
Accepted: 15-06-2024

Imad Abdul-Rida Hameed
College of Islamic Sciences, University of Kerbala, Karbala, Iraq

Jabbar S Hussein
Prosthetics & Orthotics Eng. Dep., College of Eng., University of Karbala, Karbala, Iraq

Ali A Altahir
University of Kerbala, Department of Electrical and Electronics Engineering, Kerbala, Iraq

Correspondence
Imad Abdul-Rida Hameed
College of Islamic Sciences, University of Kerbala, Karbala, Iraq

Design a grid-connected wind turbine system to feed active and reactive power to electrical load

Imad Abdul-Rida Hameed, Jabbar S Hussein and Ali A Altahir

Abstract
Optimal allocation, and robust control of generating units are essential to examine in a smart grid as the environment requires close. Researchers have paid much attention to wind energy systems in the past ten years. Utilizing renewable energy sources and micro-grids are efficient strategies for growing the reliability of a distribution system. In this study, grid utilities are simulated as a wind turbine power system with maximum power extraction, i.e., 3MW at 11 m/s wind speed and 2MW at six m/s wind speed. The renewable power system can supply a three-phase load, such as 2.5 MW. The proposed method was modeled and designed to simulate, analyze, and investigate its performance in the MATLAB Simulink environment. The SCADA system method numerically verifies load sharing for a triple-bus ring distribution network. The mathematical and simulation results demonstrate the efficient designed wind system's capacity to share load with the electrical grid. It has been concluded from this study that injecting the active and reactive with a power factor of 0.85 is required to maintain the system's stability. An increase in the reactive power was observed in the wind generator's load and the network to regulate the voltage in the transmission line.

Keywords: Boost converter, electrical grid, load sharing, renewable energy and wind turbines

1. Introduction
Fossil fuels are the most widely used resource today, and their price has skyrocketed, leading to an increase in pollution and adverse effects on the environment. These facts encourage using environmentally friendly, long-lasting renewable energy [1]. Wind power is widely used and researched and is one of the most popular renewable energy sources. A new concept and emphasis on the wind energy systems has been presented in a study [2]. Roof-mounted wind power from hidden wind farms in out-of-town homes. A small application scale wind turbine can roughly power 2.9 GWH per year per wind arrester.
A prototype wind generator report presents a characterized experiment for micro-wind farms with gains in adaptability, low noise, and 1kw generation at one m/s wind speed [3]. Hybrid wind-PV power plants can also minimize the drawbacks of integrating wind power into the grid, provide a cost-effective solution, and maximize the renewable fraction [4]. Generally, three categories of wind energy systems are domestic, stand-alone, and conventional wind turbines with ratings of 500 KW to 5 MW [5], 10-500 kW, and less than 10 kW, respectively. By synchronizing, high and intermediate-power wind turbines can supply electrical energy to the grid. Additionally, the literature depicts excessive wind connections to grid methods. Most of the time, the integrity of DC-AC and AC-DC converters is actively demonstrated in national utility-connected wind energy systems [6]. The grid-connected inverter system results in narrow DC voltage windows, high cost, and an additional control circuit for small wind turbines. Compared to conventional wind energy conversion systems, connecting a wind turbine to the grid via a single-stage matrix converter AC-AC can reduce costs, speed up power conversion, and increase system efficiency [1]. The number of renewable energy systems has significantly increased due to government incentives, technological advancements, and contributions that lower total costs. P.V. panels are widely used, but wind power is used less frequently in urban areas. The first axis wind turbine-powered EV charging station, Sanya Skypump, was constructed in Spain. In both residential and commercial settings, there is a significant rise in the demand for cutting-edge technology that offers control strategies that are quicker, less expensive, and more straightforward [7]. Renewable energy sources aren't always reliable in some countries because they depend on financial regulations and interests, but they are trustworthy in others, like Germany [8].

Residential customers are encouraged to use local power sources rather than unreliable renewable energy. Additionally, residential customers share a roof, building, and parking lot, resulting in limited space. Therefore, the best strategy is utilizing PV or wind power with a storage unit to apply renewable energy.

As a result, algorithms that make it easier to use local energy are needed, especially in situations where multiple users share energy. Due to space constraints and financial considerations, numerous customers may share renewable energy systems in the residential sector. For instance, tenants can collectively invest in a PV system in a residential building and share the generated energy. Electricity storage is the best option because electricity should be used locally, and consumption does not match generation. Personal batteries can be used to store energy and use it when it's needed, like when electricity prices fluctuate rapidly. In addition, tenants can agree to construct an electric vehicle charging station powered by wind in the community parking lot. Additionally, it is possible to envision a commercial network of wind charging stations offering a limited fixed-rate charging contract. Even though a third party owns the system, it needs an algorithm to distribute the green energy to multiple users.

The paper's main contribution is an optimization-based algorithm for dynamically changing power rates assigned to connected loads while maintaining proportional-share fairness. Users may be able to request as much energy as they want when there is a lot of it. On the other hand, when energy is a limited resource, it must be distributed based on system shares and cumulative energy consumption, favoring users who have used less energy in the past. This fairness strategy is necessary to encourage users to share an energy supply. Fair resource allocation has been studied in network engineering and computer science fields. However, power distribution from an unstable energy source is a novel subject. Examples of sources of intermittent energy include R.E.S., solar, and wind.

It could also be an excessive amount of generated power that a utility sells to a third party when demand is low under specific agreements that guarantee appropriate electricity rates, as previously mentioned. It is important to note that equitable resource distribution is a challenging objective due to the stochastic nature of user demand and the intermittent nature of energy supply. Fairness can be defined in various ways, even within the same field. Sharing power with the network and various fairness definitions, such as Min-Max fairness, potential fairness, and proportional delay minimization fairness, were discussed [9, 10].

Fairness often focuses on allocating the current resource without considering how the competing users used it in the past. Proportional-share fairness is the focus of our investigation, which assumes that a particular user has previously received a proportional share of the resource. Based on their knowledge, the researchers expect this work to be the first trial to address this kind of fair energy and power distribution. When there is excess demand, Chen *et al*. investigated two approaches for equitable power distribution to air conditioners on an intelligent grid [11]. The proposed algorithms attempt to meet their requirements as closely as possible by allocating power based on user-specified temperatures. However, the following differences exist in our work: First, the total amount of energy used by the user during the current accounting period, such as a month, is considered by our control algorithm. In addition, consumers cannot directly control the amount of power they receive, as opposed to when fairness is based on demands like a preferred room temperature. Similar to previous work in other fields [12], our objective is to distribute available energy over a more extended period through user participation in the system.

The structure of the paper is broken down in the following section. In the following section, we go into great detail about our energy-sharing system. The proposed optimization-based fairness algorithm and a few potential power allocation solutions are discussed in Section III. The simulation results and evaluation method are included in Section IV. We'll talk about some other approaches to the optimization problem before wrapping up this paper. Our conclusions are then presented in Section VI.

2. Modelling a wind energy system

The wind energy system consists of two components: An electrical generator and a wind turbine with a gearbox.

2.1 Modelling of Wind Turbine

Wind turbine uses a rotating shaft to capture airflow and turn wind energy into mechanical energy. Various input parameters, including wind speed, blade pitch angle, and others, as well as output factors like shaft speed, torque, and mechanical power, influence the energy produced by wind turbines. The following equation describes mechanical power [5]:

$$P_m = \frac{1}{2} p_a \ AV^3{}_w C_p \ (\lambda, \beta) \tag{1}$$

Where p_a is the air density at sea level at a temperature of 15 degrees Celsius:

$$p_a \ = 1.225 \text{ kg/m3} \tag{2}$$

A is the effective swept area of the blades that faces the air in the wind turbine;

$$A = \pi_{\mathrm{R}^2} \tag{3}$$

V is the wind speed; C_p is the power coefficient;
λ the tip speed ratio is given by

$$\lambda = \frac{V_r}{V_m} \tag{4}$$

V_r the blade tip speed and it is given as:

$$V_r = \frac{2\pi R}{60} n \tag{5}$$

Also, at a fixed blade pitch, the shaft speed function and wind speed are given as

$$\lambda(n, V_w) = \frac{2\pi R}{60} \frac{n}{V_w} \tag{6}$$

Where β is the blade pitch angle, which may be fixed or controllable depending on the design and capture wind force

on the blades. This study shows the pitch angle between β =104 and β =24 degrees.

Additionally, the power coefficient C_p is the ratio of the converted mechanical energy on the shaft to the energy captured from the wind by the wind turbine [9, 10].

The blade pitch angle and the number of wind turbine blades determine the power coefficient [15].

However, Betz Low restricts the power coefficient to a maximum of 0.59, which is rich. In 1919, German scientist Betz concluded that a wind turbine could not convert wind kinetic energy into mechanical power more excellent than 16/27 (i.e., 59.3%). As a result, each wind turbine's power coefficient is characterized. The following equation describes the mathematical model of the power coefficient:

$$C_p(\lambda,\beta) = c_1\left(\frac{c_2}{\lambda_1} - c_3\beta - c_4\right)exp\left(-\frac{c_5}{\lambda_1}\right)_+ c_6\lambda \quad (7)$$

Where,

$$\lambda_1 = \lambda + 0.08\beta - \frac{\beta^3+1}{0.035} \quad (8)$$

The aerodynamic constants for the power coefficient curve are c_1, c_2, c_3, c_4.

The shaft of a traditional wind turbine typically operates at a lower speed. In contrast, the modern nacelle of a widespread wind turbine houses a generator and gearbox that maintain constant conversion speeds and torque. Both sides have maintained their power: Generator and Turbine.

$$P1 = Pg \quad (9)$$

Thus,

$$T_t\omega_t = T_g\omega_g \quad (10)$$

Similarly, the mechanical torque of a wind turbine can be expressed as [5, 16], and [17].

$$\tau_g = \frac{T_t\omega_t}{\omega_g} = \frac{P_t}{\omega_g} \quad (11)$$

2.2 Modelling of synchronous generator

A three-phase synchronized generator is connected to a wind turbine. The block could be found in the Sim Power System toolbox in MATLAB. The Synchronous Generator deposits at rates sufficient to supply a maximum load of 2 MW at 50 Hz and 11 kV. The output terminal voltage's level could be fixed by employing an excitation block. In [18] and [19], the generator's d-q model equations are modeled and discussed. Electromechanical energy conversion is when a generator transforms mechanical energy into electrical energy. The mechanical model of a synchronous generator can be found below;

$$\Delta\omega(t) = \frac{1}{2H}\int_0^t (T_m - T_e)dt - K_d\,\Delta\omega(t) \quad (12)$$

$$`(t) = \Delta\omega(t) + \omega_o \quad (13)$$

Table 1 displays the rated parameters and specifications of the W.E.S. (wind turbine and electrical generator) modeled for the current study.

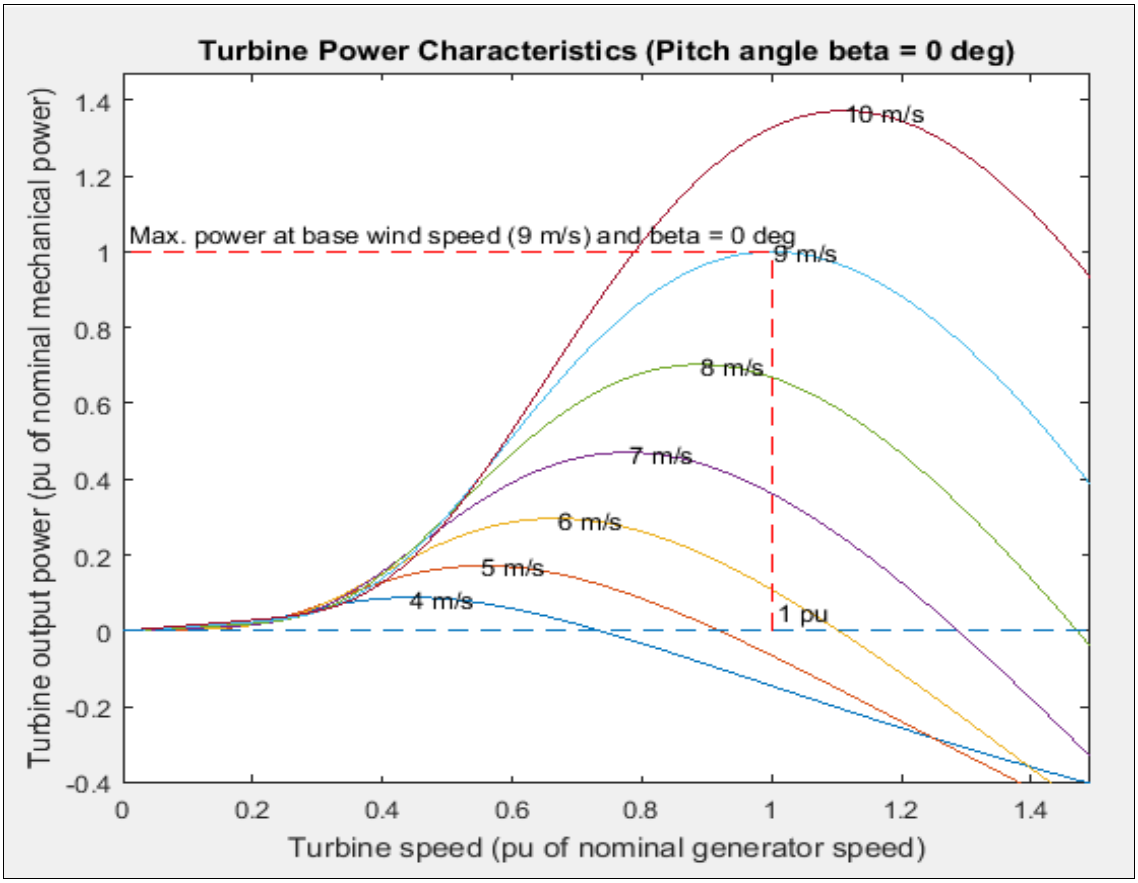

Fig 1: Wind turbine power speed characteristics

Table 1: Displays the rated parameters and specifications of the W.E.S. (wind turbine and electrical generator) modeled for the current study

Generator Parameters	Values
Nominal power, lin-to-lin voltage, Frequncy [Pn(VA), Vn(V_{rms}), fn(Hz)]	[3.3, 575, 50]
Stator [R_S, L_{IS}] (pu)	[0.004843, 0.1248]
Rotor [R_S, L_{IS}] (pu)	[0.004377, 0.1791]
Magnetizing inductance Lm (pu)	6.77
Turbine Parameters	Valus
Pitch angle beta used to display characteristics (beta≥0) deg	0
Pitch angle controller gain [kp, ki]	[5, 25]
Maximum pitch angle (deg)	45
Maximum Rat of change of pitch angle (deg/s)	2
Nominal wind turbine mechanical output powe (w)	3×10^6
Base wind speed (m/s)	9
Base rotational speed (pu of base generator speed)	1

2.3 Modeling of national grid supply

In this case study, 132 kV grid stations are proposed to commission the national grid. These stations supply an 11 kV substation via a 25 km 132 kV transmission line. Through 132 kV/11 kV transformers, the voltage is reduced to 11 kV at the 11 kV substation. The load to the customer is guaranteed by the distribution line, or power supply, with a length of 5 km and a voltage of 11 kV. During unloading times and peak hours, the consumer receives 6 MW of charging power from the national grid.

2.4 Variable electrical load modeling

Consumer side loads, also known as electrical loads on both systems, are provided by the Variable Electrical Load (VEL) Modeling W.E.S. NGS. There are two parts to the time-varying load known as VEL: Peak load of 2 M.W. and base load of 6 M.W. Throughout both peak and off-peak hours, the fundamental components of the VEL remain permanently connected to bus B3. The three-phase circuit breaker only switches the VEL's peak load component during peak load times. The circuit breaker opens or closes when the load management unit sends a signal. Figure 6 depicts the load profile analyzed in this case study.

2.5 Load management unit

The Load Management Unit (L.M.U) enables the fuzzy logic controller to sense changes in load and direct the W.E.S. to take on extended load demands during peak load periods. L.M.U. also determines and sends operating conditions for W.E.S., VEL, and Fuzzy Logic Controllers. Before this, the L.M.U specified the load switching interval for the VEL to turn on or off the peak load component. Therefore, L.M.U functions analogously to a centralized control system that coordinates with the entire system and directs it to act accordingly [1].

2.6 Boost converter module

The maximum power objective is to modify the DC-DC control variables. One of the methods available for MPP achievement tracking. Perturbation and Observation, Incremental Conductance Technique (I.C.T.), Perturbation and Observation, and Current-Based Maximum PowerPoint Tracker. The constant reference method is utilized in this article. A continuous reference voltage (or current) corresponding to the wind turbine voltage (or current) at the maximum power point under specific atmospheric conditions is used in standard MPPT techniques to compare the wind turbine. The power conditioner is driven by the difference signal, also known as the error signal, which connects the wind turbine to the load. The technology isn't very accurate because it doesn't account for the effects of temperature and irradiance changes or the difficulty of choosing the best point, as shown in Figure 1 [20]. A boost converter can be utilized for precise M.P.P. tracking, as stated in [20]. A boost converter is a DC-to-DC voltage converter that emphasizes the output DC voltage more than the input DC Voltage. It consists of at least two semiconductor switches: A diode that acts as a freewheeling diode to ensure the path of the current in other controlled off states and a transistor that connects the source voltage in series). In the converter's output stage, capacitor and inductor filters reduce voltage and current ripple, respectively. A converter's fundamental operation is based on two distinct states. The inductor current is increased when the switch is closed in one configuration. The inductor current decreases when the button is turned on in the off state. The following describes the boost converter's performance [21]:

$$V_{dc} = \frac{V_{wind}}{1-D} \tag{14}$$

$$I_{dc} = (1-D) I_{wind} \tag{15}$$

The result of dividing Equation (*1*4) by Equation (*1*5) is as follows:

$$R_{in} = (1-D)^2 R_o \tag{16}$$

Where D is the boost converter's duty cycle ratio, and $t_{on} = D * Ts, t_{off} = (1-D)\, Ts$.

2.7 Three-phase pulse width modulation inverter

This study uses a three-phase pulse width modulation inverter with a voltage source. The following equation describes the inverter's performance. Harmonics that cause the inverter current to enter the grid are reduced when the three-phase inverter is connected to the LCL filter. It has not examined the filter's subject in this study, but one can check it in other studies [20]:

$$V_{LL,RMS} = 0.6124\, m\, V_{dc} \tag{17}$$

Where, $m = V_{Peek\ Control\ Signal} / V_{Peak\ Triangle\ Signal}$

2.8 Formulation of problem

2.8.1 Objective Functions

The main purpose of the proposed scenario is to ascertain the optimal location and capacity of Distributed Generators

(DGs) in order to achieve the most favorable objective function, which involves minimizing power losses and voltage fluctuations, while also adhering to operational constraints. The true losses can be expressed in the following manner [23]:

$$V_i = \sum_{i=1}^{NPQ} |VD - 1| \quad (18)$$

NPQ represents the count of load buses, VI denotes the amount of voltage at bus i, and VD represents the overall voltage fluctuation at the load buses. The definitions of the minimal loss function and power loss are provided in (19), and (20).

$$Min(f_1) \triangleq \sum_{i=1}^{NB} P_{loss},$$

$$f_1 \triangleq \frac{\sum_{i=1}^{L} P\ loss\ (i) after\ inserting\ DGs}{\sum_{i=1}^{L} P\ loss\ (i) befor\ inserting\ DGs} \quad (19)$$

where L is the number line in the distribution network and power losses can be defined as in (21):

$$P_{loss} = \sum_{i=1}^{N} \sum_{j=1}^{N} \left(\alpha_{ij} \left(P_i P_j + Q_i Q_j \right) + \beta_{ij} \left(Q_i P_j - P_i Q_j \right) \right) \quad (20)$$

P_i, P_j are the total effective active and reactive power supplied behind the bus i, j.
The real and imaginary power in bus i are calculated based on the generation and demand power, as specified in the given definition (21):

$$P_i = P_{G_i} - P_{D_i}, \quad Q_i = Q_{G_i} - Q_{D_i} \quad (21)$$

The constant design parameters between bus I and j are defined as in (22), (23):

$$\alpha_{ij} = \frac{r_{ij}}{v_i v_j} \cos(\delta_i - \delta_j) \quad (22)$$

$$\beta_{ij} = \frac{r_{ij}}{v_i v_j} \cos(\delta_i - \delta_j) \quad (23)$$

And the line impedance is defined as in (24):

$$r_{ij} + jx_{ij} = z_{ij}, \quad [Z_{bus}] = [Y_{bus}]^{-1} \quad (24)$$

Where, $ij'th$ element of bus impedance matrix, $[Z_{bus}]$ is:

2.8.2 Constraints

Within this paragraph, the subsequent limitations are applicable to certain goal functions in the following manner:

a) **Electricity balance constraint:** The total sum of electricity flowing into and out of the distribution network must be equal [23].

$$\sum_{i=2}^{n} P_{DG_i} \leq \sum_{i=2}^{n} P_i + \sum_{i=1}^{b} P_{loss_{i \to i+1}} \quad (25)$$

b) **Voltage constraint:** The magnitude of the voltage at each bus must be limited by the following equation:

$$|V_1 - V_i| \leq \Delta V_{\max} \qquad \forall i = 1, 2, \ldots n \quad (26)$$

c) Thermal limit

$$|J_i| \leq J_{i\max} \quad (27)$$

Where, J_{imin} is the minimum thermal limit at bus *i*.
The thermal limit is determined by calculating the current passing through each branch. The objective function imposes a penalty for any violation of the inequality requirements. The voltage stability index (VSI) is defined as shown in (28) [23]:

$$VSI(k) = |V_i|^4 - 4(P_k . X_{ik} - Q_k . R_{ik})^2 - 4(P_k . R_{ik} + Q_k . X_{ik})^2 |V_i|^2 \quad (28)$$

f_2 Displays the improvement of the Voltage Stability Index (VSI). Then f_2 can be expressed as:

$$f_2 \triangleq \frac{1}{VSI(k)_{with\ DGs}} \quad (29)$$

f_3 Presents the improvement of voltage profiles and it can be expressed as in (30):

$$f_3 \triangleq \frac{\sum_{i=1}^{N} |V_i - V_{ref}|_{with\ DGs}}{\sum_{i=1}^{N} |V_i - V_{ref}|_{without\ DGs}} \quad (30)$$

The multi DGs locations and their sizing can be obtained optimally by solving (31) [24]:

$$f_{total} = w_1 f_1 + w_2 f_2 + w_3 f_3 \quad (31)$$

Where, w_1, w_2 and w_3 are weighting factors. The sum of the absolute values of these weights assigned to all impacts should add up to one as shown in (32):

$$|w_1| + |w_1| + |w_1| = 1 \quad (32)$$

In this research, the value of w_1 is set to 0.5, whereas both w_2 and w_3 are set to 0.25. The significance of the active power losses has increased due to the level of worry around them.

3. Results and Discussion

The case study simulation diagram has been completed by modeling WES, NGS, LMU, and VEL. As can be seen in Figure 1, the single system diagram serves as the basis for the comprehensive modeling. The WES is picked up when it senses load. The case study says that WES shares the extensive load component during peak times, while NGS

always meets the 3 MW load demand. All the WES, LMU, NGS, and VEL models have been implemented using Simulink. The information the LMU needs to communicate with the other simulation subsystems is provided. Commands for peak occurrence and peak fall instants, in addition to rates of change for maximum occurring and maximum drop during both peak and off-peak hours, are included in this data set. Figure 2 shows single line diagram for three buses distribution network.

It has been shown that the load has a power factor of 0.8576 and an adequate capacity of 1.217Mvar, respectively, as shown in Figure 3. The following research and results demonstrate that the wind generator will supply this load by altering the wind speed. The generation of effective power P is between (2-3) MW of adequate power. In the event of a sudden change in wind speed, we observe a generation disturbance, so there are two instances. The first is when the rate changes from low to high; in this case, we see an increase in a random generation that cannot be controlled, and the generated current and voltage are not in phase with one another, resulting in a negative power factor. The second scenario is when the speed changes from high to low. In this instance, one observes the system's overall instability.

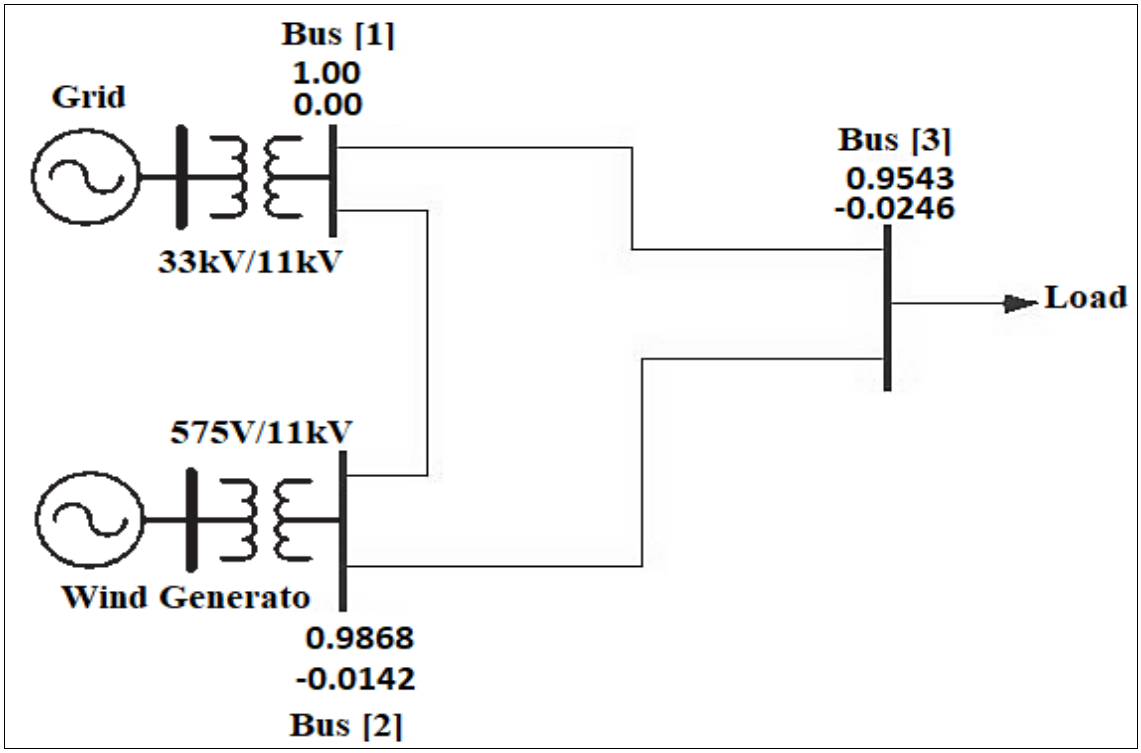

Fig 2: Single line diagram for three bus distribution network

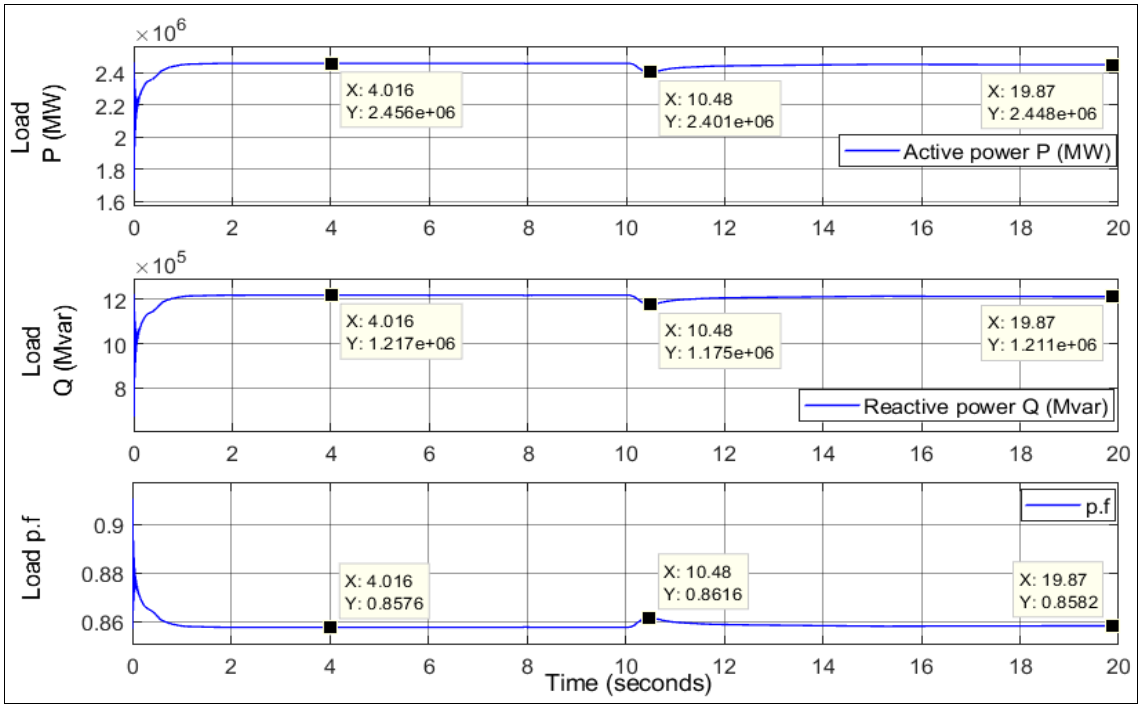

Fig 3: Time response for active and reactive power for the load with load power factor.

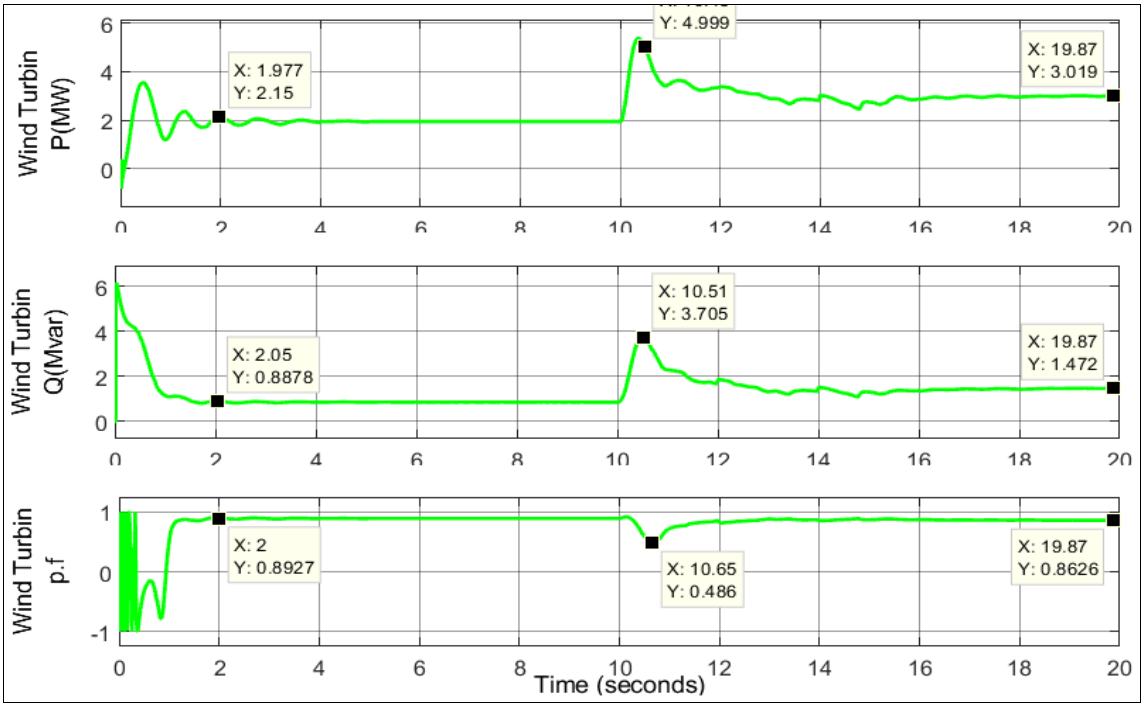

Fig 4: Active and reactive power for the wind turbine with its power factor.

It has been noted that the ineffective capacity is controlled through the filter and thus raises its to help in preparing the load with a power factor equal to 0.85, as shown in Figure (3), to reduce the withdrawal of the ineffective capacity from the national network and thus to maintain the power factor of the network National within the specified range 0.95. The power factor of the wind generator is 0.89, which is arguably ideal for load processing. The line voltage is stable in all cases of (0.9868-0.9843), while in the case of moving at wind speed from (6-11) m/s, it is at (0.9699), and this means that the voltage is stable in all cases.

The second section of Figure (5) depicts the transmission line's ineffective power. The stability of the Q has been noted to be from (1.3 to 1.5 Mvar), while the ineffective power is at the importance of (2.9 Mvar).

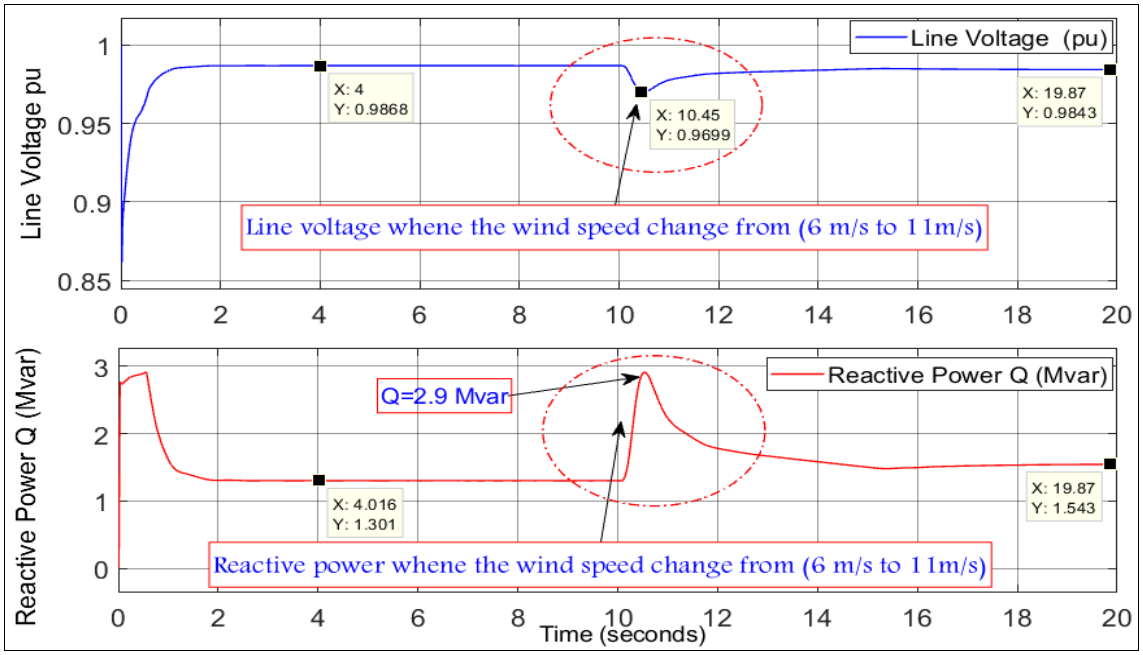

Fig 5: Line voltage and reactive power for the power system

The load sharing between the wind generator and the network is depicted in Figure 6. The following particulars are visible. At a wind speed of 6 m/s, we observe that the load requires real power (P_{Load} = 2.456 MW) and that the wind generator supplies an absolute control of (P_{Wind} = 2.03 MW). The network will compensate for this lack of equipment by only providing (0.4148MW) the following equation. The compensative active power from the grid is P_{Load} = 2.45MW. When the wind speed is (11 m/s), we notice that the wind generator supplies real power (P_{Wind} = 3.019MW) and that the load requires real power, P_{Load} = 2.456MW. The compensative active power from the grid is

P_{Load}, which is equal to P_{grid}, P_{wind}, 2.031MW, 0.4148MW, and 2.45MW. The following equation can be used: P_{grid} = 0.54MW. The curve appears to be out of balance. The sudden change in wind speed is the reason. The subsequent research will offer suggestions for solutions.

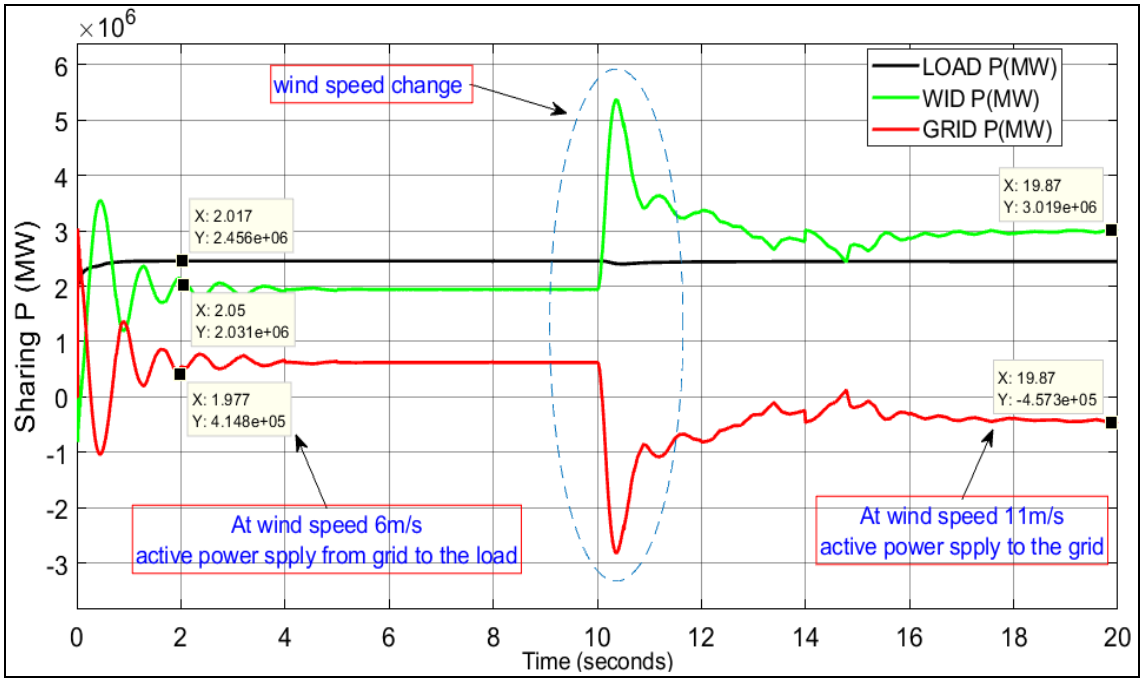

Fig 6: Load sharing (Active power) between the wind generator and grid.

The load sharing between the wind generator and the network is depicted in Figure (6). At a wind speed of 6 m/s, one observes that the load requires a reactive capacity and the wind generator supplies reactive power at 0.88 Mvar. The network will compensate for the lack of equipment with (0.5623) Mvar. An increase in the reactive power was observed in the wind generator's load and the network to regulate the voltage in the transmission line. This corresponds to the compensative active power from the grid, which is $Q_{Load} = Q_{grid} + Q_{wind}$ = 1.4423MW. At a wind speed of (11 m/s), we observe that the wind generator is preparing reactive power (Q_{Wind} = 1.47 Mvar) and that the load requires reactive power (Q_{Load} = 1.2 Mvar).

As a result, we observe an increase in the processing of (0.25 MW) that will be injected into the network by following the equation. $Q_{grid} = Q_{wind} - Q_{Load}$ = 0.25 Mvar. An increase in the reactive power supplied to the load by the wind generator and the network has been observed to regulate the voltage in the transmission line. The sudden change in wind speed is the reason. The subsequent study will offer suggestions for solutions.

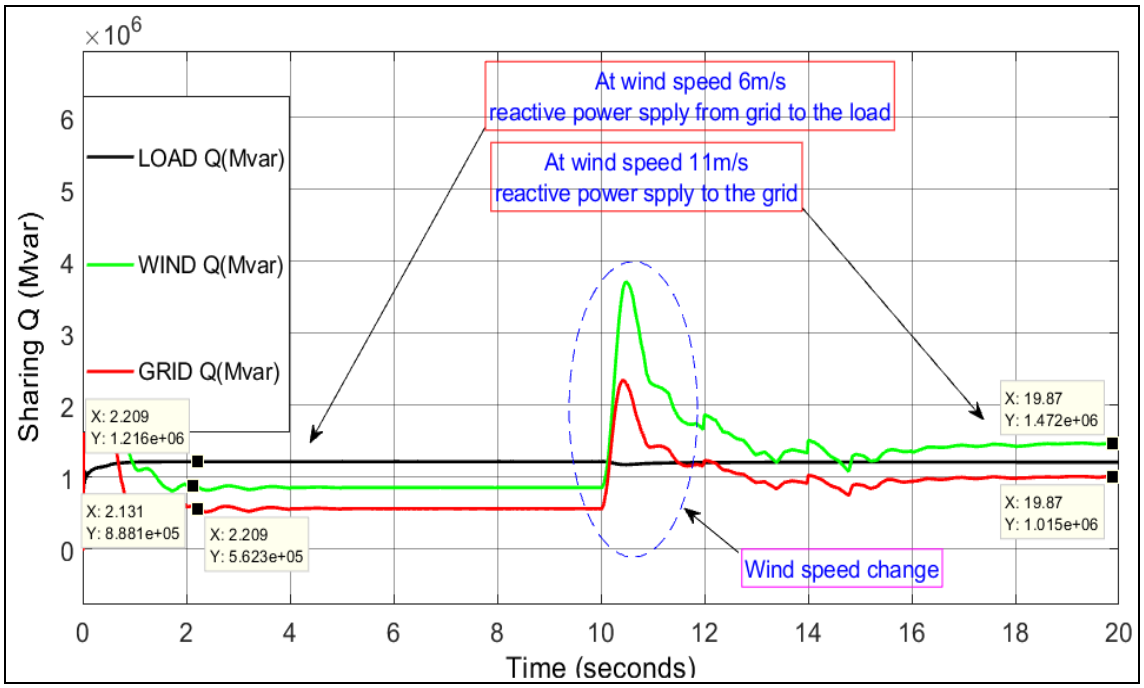

Fig 7: Load sharing between the wind generator and grid.

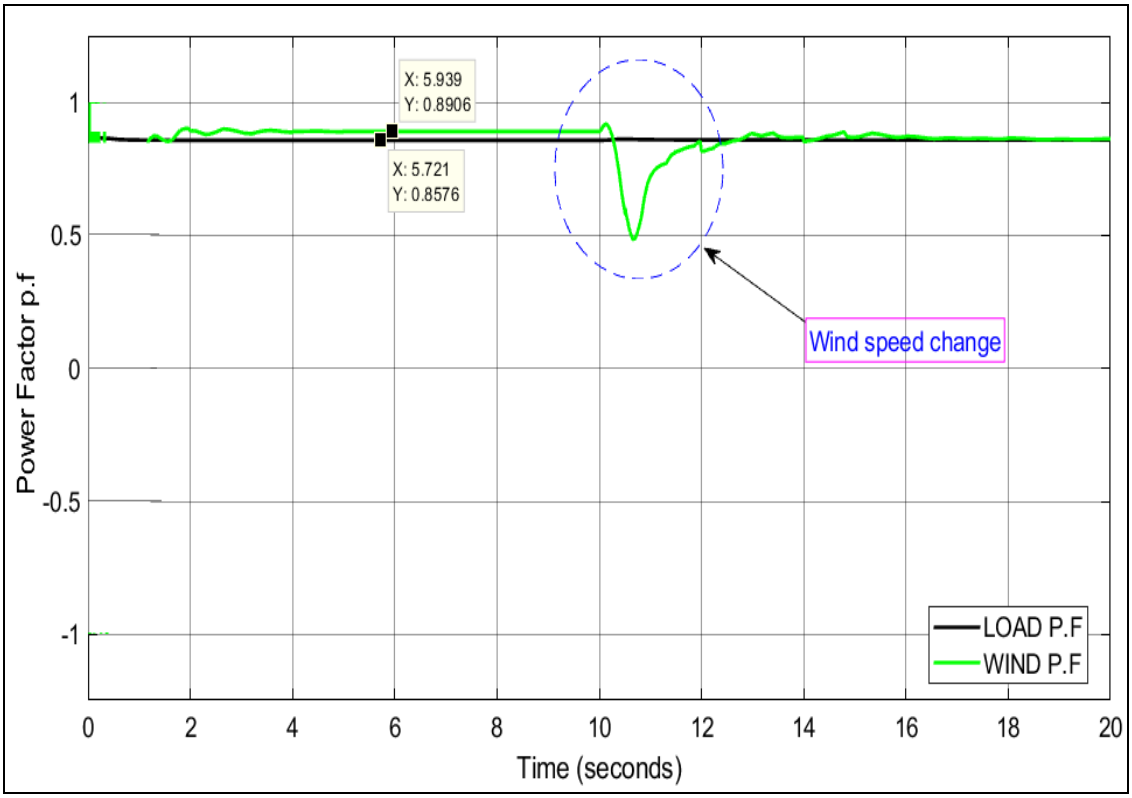

Fig 8: Time response of power factor for wind generator.

4. Conclusions

A distributed wind generation system is presented in this paper to meet the increased energy consumption during peak times. Additionally, it participates in the electricity market and contributes to the nation's economy without using electrical components like converters or inverters. However, the erratic nature of wind energy's contribution to supply may increase costs, emissions, and efficiency due to the frequent need to switch to a large number of other plants so that even when the wind stops, demand remains high**.**

In contrast, wind turbines are a non-disposable source of electricity generation. Meteorological methods can only predict the wind speed and the amount of power produced, but there is no way to influence the availability of renewable resources. The electric supply system must adapt to the characteristics of offshore wind if the possibilities of these renewable sources are to be utilized effectively. Wind turbines generate electricity based on the available wind velocity. Therefore, sophisticated management of the steam power plant is required to integrate wind energy into an existing power system effectively. This article focuses on how integrating renewable power affects the reliability of such an electric power grid. The dependability of wind turbine electricity generation has been quantified using a capacity credit**.**

By injecting the national grid system, it was injecting the active and reactive from the wind generator, where it is applicable to inject the hypnotic with pure power from the generation of renewable energies, leading to a high frequency of the hypnotized relative to demand. It has been concluded from this study that injecting the active and reactive with a power factor of 0.85 is required to maintain the system's stability.

5. References

1. Ashraf MM, Waqas AB, Malik TN. Grid connected wind energy conversion system for peak load sharing using fuzzy logic controller. Int J Renew Energy Res. 2017;7(4).
2. Amini A, Kamoona M. Hidden wind farms potential for residential households having roof-mounted wind arrester. In: Renewable Energy Research and Application (ICRERA), 2014 International Conference On; c2014, 891-896.
3. Caruso M, Di Tommaso A, Genduso F, Miceli R, Galluzzo GR, Spataro C, *et al*. Experimental characterization of a wind generator prototype for sustainable small wind farms. In: Renewable Energy Research and Applications (ICRERA), 2016 IEEE International Conference on; c2016, 1202-1206.
4. Kiymaz Ö, Yavuz T. Wind power electrical systems integration and technical and economic analysis of hybrid wind power plants. In: Renewable Energy Research and Applications (ICRERA), 2016 IEEE International Conference on; c2016, 158-163.
5. Anaya-Lara O, Jenkins N, Ekanayake J, Cartwright P, Hughes M. Wind Energy Generation Modelling and Control. West Sussex, United Kingdom: John Wiley & Sons, Ltd; c2009.
6. Kamali ZH, Salameh Z, Ashfaq A. Modeling of wind energy conversion system using PSCAD/EMTDC. Int J Renew Energy Res. 2017;7:178-187.
7. Etinski M, Schulke A. Fair Power Allocation in Multi-User Systems with Controllable Loads. In: IEEE smart grid Comm 2013 Symposium Architectures and Models for the Smart Grid.
8. Fulton M, Capalino R, Auer J. The german feed-in tariff: Recent policy changes. Deutsche Bank Research; c2012.
9. Massouli'e L, Roberts J. Bandwidth sharing: Objectives and algorithms. IEEE/ACM Trans Networking. 2002;10(3):320-328.

10. Demers A, Keshav S, Shenker S. Analysis and simulation of a fair queuing algorithm. ACM SIGCOMM Comput Commun Rev. 1989;19(4):1-12.
11. Chen YW, Chen X, Maxemchuk N. The fair allocation of power to air conditioners on a smart grid. IEEE Trans Smart Grid. 2012;3(4):2188-2195.
12. Kay J, Lauder P. A fair share scheduler. Commun ACM. 1988;31(1):44-55.
13. Ashraf MM, Malik TN, Iqbal M. Peak load sharing based on blade pitch control of wind turbine in the presence of utility supply. J Renew Sustain Energy. 2014;6:013110.
14. Joshi S, Patel A, Patel P, Patel V. Wind Energy - A Brief survey with wind turbine simulations. Int J Comput Commun Inf Syst. 2010;2:228-232.
15. Lain S, Quintero B, López Y. Aeromechanical evaluation of large HAWT's blades. J Sci Ind Res. 2010;69:142-145.
16. Evren S, Ünel M, Akşit MF, Tuzla I. Modeling and control of a variable speed variable pitch angle prototype wind turbine. Math Comput Appl. 2013;18:408-420.
17. Gilev B, Slavchev J, Penev D, Yonchev A. Model and predictive control for a wind turbine. In: Proceedings of A.I.P. Conference; c2011, 15.
18. Krause PC. Analysis of Electric Machinery. New York: McGraw Hill; c1986.
19. Kamwa I, Pilote M, Viarouge P, Mabwe MB, Crappe M, Mahfoudi R. Experience with computer-aided graphical analysis of sudden-short-circuit oscillograms of large synchronous machines. IEEE Trans Energy Convers. 1995;10:407-414.
20. Rashid MH. Electronics Handbook Devices, Circuits, and Applications. 3rd Ed. Elsevier; c2011.
21. K.H. Turkey. Application of quasi-Z-source inverter in photovoltaic grid-connected system. J Eng Sustainable Dev. 2017;21(2):103-105.
22. Hameed IA. Load sharing regulation of a grid-connected solar photovoltaic system in Karbala city. J Eng Sustainable Dev. 2018;22(2):168-181.
23. Prabha DR, Jayabarathi T, Umamageswari R, Saranya S. Optimal Location and sizing of distributed generation unit using intelligent water drop algorithm. Sustain Energy Technol Assess. 2015;11:106-113.
24. Ali ES, Elazim ASM, Abdelaziz AY. Ant lion optimization algorithm for renewable distributed generations. Energy. 2016;116:445-458.

Appendix

Table 1: Generation, loads and bus voltage for three bus grid at wind speed 11m/s

Table: 1.2 at wind speed 11m/s						
Bus No.	**Bus Voltage**	**Generation MW**	**Generation MVAR**	**Load MW**	**Load MVAR**	**P.F**
1.	1.04+j0.0	-0.4573	1.015	0	0	1
2.	1.02+j0.0	3.019	1.47	0	0	0,8576
3.	1.00+j0.0	0	0	2.5	1.216	0,8778

Table 2: Generation, loads and bus voltage for three bus grid at wind speed 6m/s

Table: 1.2 at wind speed 6m/s						
Bus No.	**Bus Voltage**	**Generation MW**	**Generation MVAR**	**Load MW**	**Load MVAR**	**P.F**
1	1.03+j0.0	0.4248	0.5623	0	0	1
2	1.012+j0.0	2.031	0.8881	0	0	08906
3	1.01+j0.0	0	0	2.5	1.21	0.8576